ELSEVIER

Cement & Concrete Composites 25 (2003) 851–855

Cement & Concrete Composites

www.elsevier.com/locate/cemconcomp

Extent of immiscibility in the ettringite–thaumasite system

S.J. Barnett [a,*], D.E. Macphee [a], N.J. Crammond [b]

[a] Department of Chemistry, University of Aberdeen, Meston Walk, Aberdeen AB24 3UE, UK
[b] Centre for Concrete Construction, BRE, Garston, Watford WD25 9XX, UK

Abstract

Solid solutions between thaumasite and the related phase ettringite were prepared and characterised by X-ray diffraction and infrared spectroscopy. A miscibility gap in the solid solution is identified and defined. Crystallographically, the miscibility gap is identified as a gap in the unit cell dimensions of the solid phases formed between $c \cong 20.95$ (10.475) and $c \cong 21.3$ Å. A combination of quantitative X-ray powder diffraction and infrared spectroscopy enabled us to define the miscibility gap in terms of Al:Si ratio. Ettringite can accept the replacement of 1/2 its Al by Si, while thaumasite tolerates little or no Al in its structure.
© 2003 Elsevier Ltd. All rights reserved.

Keywords: Thaumasite; Ettringite; Solid solution

1. Introduction

Thaumasite ($Ca_3SiSO_4CO_3(OH)_6 \cdot 12H_2O$) and the related phase ettringite ($Ca_6Al_2(SO_4)_3(OH)_{12} \cdot 26H_2O$) are formed in cement and concrete by the action of aqueous sulfates and/or carbonates [1–4]. The formation of ettringite is limited by the alumina content of the cement and leads to expansion and cracking. The effects of thaumasite formation can be much more severe since it involves the reaction of the main binding phase of the cement, calcium silicate hydrate (C–S–H). Thaumasite (Fig. 1) and ettringite have very similar structures and therefore give similar X-ray diffraction (XRD) patterns. The identification of the thaumasite form of sulfate attack (TSA) by XRD can therefore be problematic and it is likely that in the past TSA has been incorrectly diagnosed as conventional sulfate attack, in which ettringite is produced.

The structure of thaumasite [5] (depicted in Fig. 1) is based on columns with composition $[Ca_3Si(OH)_6 \cdot 12H_2O]^{4+}$. The sulfate and carbonate anions lie in an ordered arrangement in channels between the columns. The structure is hexagonal with $a = 11.054$ Å and $c = 10.410$ Å [5,6]. Ettringite has a similar structure [7] with silicon replaced by aluminium and sulfate plus carbonate replaced by sulfate plus $2H_2O$ in the channels. It has lower symmetry with a trigonal lattice and the c-dimension approximately doubled ($a = 11.23$ Å, $c = 21.50$ Å [6,7]). The change in symmetry is apparently caused by the ordering of the anions in the channels of the two structures. The charge difference of Si and Al means that the total charge of anions required in the structure is reduced in ettringite.

The similarity of the crystal structures of thaumasite and ettringite leads to the possibility of the formation of solid solutions between them. This solid solution has been discussed in the literature [5] and observed in natural samples [8], concrete affected by TSA [2] and laboratory studies [9,10]. A miscibility gap is expected to exist [5,10] because of the different symmetries of the two structures. However, no information is available on the extent of the miscibility gap.

In this paper, the characterisation of thaumasite–ettringite solid solutions by X-ray diffraction and infrared spectroscopy is described. Other work on these phases is described separately [11–13].

2. Preparation of materials

Solid solutions between thaumasite and ettringite were prepared by mixing a slurry of calcium oxide in

* Corresponding author. Address: Department of Civil Engineering, University of Liverpool, Brownlow Street, Liverpool L69 3GQ, UK. Tel.: +44-1224-272941; fax: +44-1224-272921.

E-mail addresses: barnett@liv.ac.uk (S.J. Barnett), d.e.macphee@abdn.ac.uk (D.E. Macphee).

0958-9465/$ - see front matter © 2003 Elsevier Ltd. All rights reserved.
doi:10.1016/S0958-9465(03)00116-1

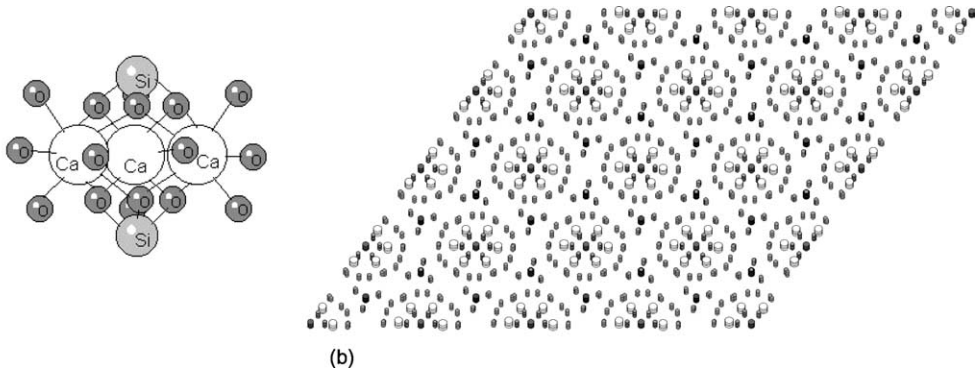

Fig. 1. Crystal structure of thaumasite (a) column structure lying parallel to *c*-axis (b) projection of structure onto *ab* plane.

10% sucrose solution with one of the appropriate amounts of sodium silicate, sodium aluminate, sodium carbonate and sodium sulfate [6,10].

Both the silicon:aluminium and sulfate:carbonate ratios in the starting mixes were varied in 10% increments between the thaumasite ($Ca_3SiSO_4CO_3(OH)_6 \cdot 12H_2O$) and ettringite ($Ca_6Al_2(SO_4)_3(OH)_{12} \cdot 26H_2O$) compositions. The mixes were sealed in polyethylene bottles and stored at 5 °C for 6 months with periodic agitation, prior to isolation by suction filtration. In order to prevent contamination by atmospheric carbon dioxide, preparation and isolation were carried out under nitrogen. All water used was double distilled, boiled and cooled under nitrogen before use.

X-ray diffraction was carried out shortly after isolation in order to determine unit cell parameters and the results are described in a separate paper [11]. For the work described here, quantitative X-ray diffraction and infrared spectroscopy were carried out 18–24 months later, after the solids had been stored dry in sealed plastic bags. Transmission electron microscopy, energy-dispersive X-ray analysis and electron diffraction studies of these solids are described elsewhere [11–13].

3. X-ray diffraction

X-ray diffraction and Rietveld refinement were used to obtain accurate unit cell dimensions for the solid solution phases produced, and quantitative phase information. Solids were prepared for analysis by lightly grinding with corundum (α-Al_2O_3) in a 1:1 weight ratio, and side-loading into the sample holder to minimise preferred orientation. X-ray diffraction data were collected on a Bruker AX8 diffractometer, using CuKα radiation over the angular range 5–60° 2θ, with a step size of 0.04° and a count time of 4 s per step. Rietveld refinement was performed using the general structure analysis system (GSAS) software [14,15]. Unit cell parameters, 2θ-zero errors, scale factors, peak shape and width parameters were refined. Atomic positions were not refined since the data quality was not considered to be adequate. A more detailed description of the refinement procedure is given elsewhere [12], along with a graph showing the quality of fit of observed and calculated data.

The results from QXRD are shown in Figs. 2 and 3. Fig. 2 shows the unit cell parameters of the solid solution phases present, with *c* plotted against *a*. Fig. 3 shows the quantitative phase information obtained for the solids from the Rietveld refinement results. In many cases, two solid solution phases coexist, one similar to ettringite and one similar to thaumasite.

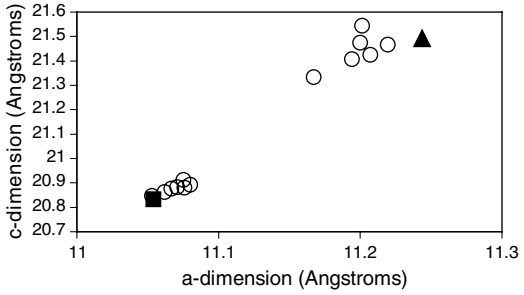

Fig. 2. Unit cell parameters of solid solution phases: square, thaumasite; triangle, ettringite; circle, solid solution phases.

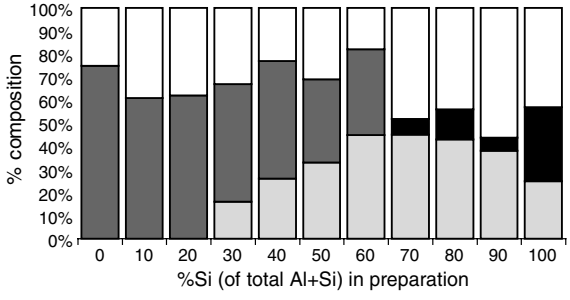

Fig. 3. Quantitative XRD results: pale grey, thaumasite; dark grey, ettringite; black, calcite; white, amorphous phase.

In Fig. 2, a gap exists between the unit cell dimensions of the two structure types. We believe that this gap corresponds to a change in symmetry between thaumasite and ettringite. Solid solutions with $c > 21.3$ Å are characterised as ettringite-like structures, while phases with $c < 20.95(10.475)$ Å are characterised as thaumasite-like structures. There is no significant change in unit cell parameters since the solids were first analysed by X-ray diffraction [11].

Quantitative phase information (Fig. 3) shows that the solids contain contaminating phases, i.e. calcite and an amorphous phase, likely to be calcium silicate hydrate. In samples close to the thaumasite end of the series, the amount of amorphous material present increases sharply and calcite is formed. There is no significant change in relative amounts of the two solid solution phases since the solids were first isolated [11].

4. Infrared spectroscopy

Fourier transform infrared spectroscopy was carried out using an ATI Mattson Genesis Series FTIR transmission instrument. A known mass of solid was ground with dried KBr and the mixture was pressed at 2000 psi for 5 min. Infrared data were collected over the wavenumber range 400–4000 cm^{-1}. The infrared spectra of some of the solids are shown in Fig. 4. The absorption bands present in these spectra were identified by comparison with previously published data for thaumasite and ettringite [16–19], and by reference to other more general work [20,21]. Table 1 identifies some of the important bands in the IR spectra of these materials.

Infrared data analysis was carried out using Microsoft Excel®. A procedure was devised to quantify the octahedral Si bands in the spectra. The experimental absorption spectrum was fitted by least-squares methods to a calculated spectrum produced by mixing the experimental spectra of the ettringite and thaumasite end members:

$$I_{ci} = X(I_{ei}) + Y(I_{ti})$$

where I_{ci} is the calculated absorbance at wavenumber i, I_{ti} and I_{ei} are the measured absorbances of thaumasite and the ettringite respectively at wavenumber i, and X and Y are variables. The thaumasite spectrum used in the calculated pattern is a high purity natural sample from Crestmore, California. The fitting was performed over the wavenumber range 475–525 cm^{-1} (corresponding to the 500 cm^{-1} SiO_6 band) by varying X and Y, and a good quality of fit was achieved over the whole spectrum (see Ref. [12]). Since only thaumasite (I_{ti}) contributes to the intensity of this band in the calculated pattern, the value of Y is proportional to the amount of octahedral Si present in the solid.

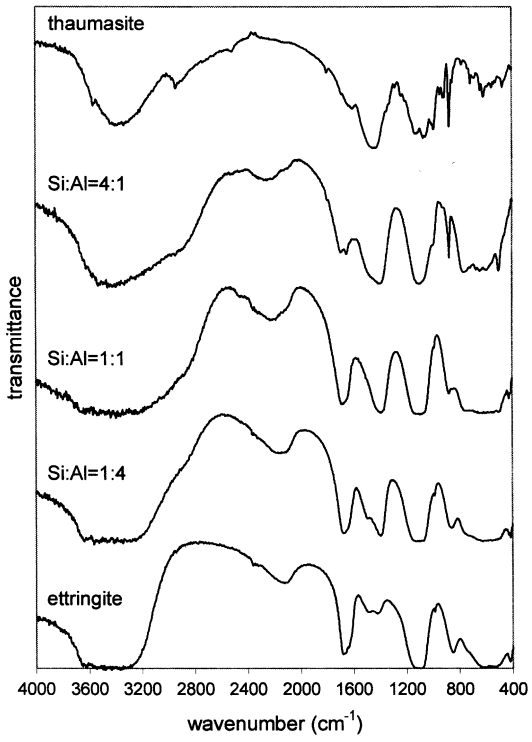

Fig. 4. Infrared spectra of selected solids. Note: Si:Al ratios refer to the molar ratios in the starting mixes.

Table 1
Wavenumbers of important infrared absorption bands

Wavenumber/cm^{-1}	Assignment
3600–3200	O–H stretch
1680	O–H bend
1400	C–O stretch (CO_3^{2-})
1100	S–O stretch (SO_4^{2-})
940/920	SiO_4
875	C–O bend (CO_3^{2-})
850	AlO_6
750	SiO_6 stretch
500	SiO_6 bend

In order to account for the presence of other phases in the solid, and hence obtain a measure of octahedral Si in the solid solution phase, these results were normalised with the quantitative XRD data described above using the equation:

$$\text{moles octahedral Si in ettringite/thaumasite} = Y * \frac{\text{moles}_{\text{std}} * \text{mass}_{\text{std}}}{\text{mass}_{\text{e/t}}} * \frac{\text{MW}_{\text{e/t}}}{\text{MW}_{\text{std}}}$$

where $\text{moles}_{\text{std}}$ is the number of moles octahedral Si in 2 moles of standard thaumasite = 2, mass_{std} is the mass of standard, $\text{mass}_{\text{e/t}}$ is the mass of ettringite/thaumasite in the sample (calculated from the measured total mass of the sample and the QXRD crystallinity)

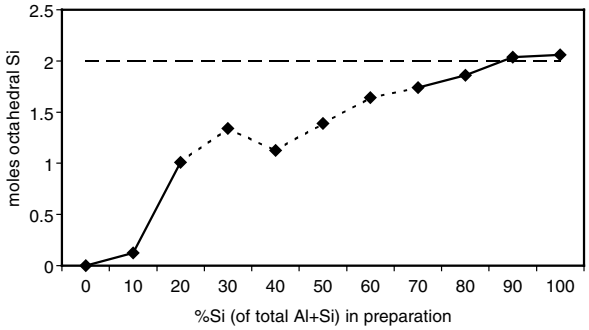

Fig. 5. Octahedral Si levels in solid solutions: solid diamond, measured values (dotted line indicates two-phase region); dashed line, theoretical maximum (i.e. thaumasite composition).

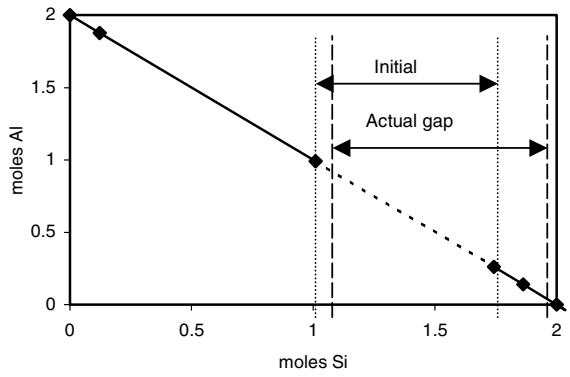

Fig. 6. Extent of immiscibility in the thaumasite–ettringite system: dotted line, two-phase region; solid line, "single"-phase region; diamond, measured compositions of single-phase systems.

and $MW_{e/t}/MW_{std}$ is the ratio of molecular weights of standard and sample (≅1).

The Si contribution to the solid solution composition relative to the starting compositions is shown in Fig. 5. The dotted region of this graph represents the solids in which two ettringite/thaumasite phases formed. In these cases, the value plotted represents an average of the octahedral silicon contents of the two solid solution phases. These two-phase systems are mixtures of the two compositions representing the miscibility limits of the solid solution.

As an initial estimate of the miscibility limits, it was assumed that the compositions of the single-phases on either side of the two-phase region represented the limits of the solid solution. The two-phase systems would therefore be mixtures of these two compositions. This would suggest that ettringite can accept the replacement of up to 1/2 its aluminium by silicon, while thaumasite tolerates the replacement of 1/8 of its silicon by aluminium.

A more detailed approach was then used to calculate the miscibility limits from the average values for the two-phase systems, using the following equation:

$$n(\mathrm{Si_{oct}}) = f_{\mathrm{ett}} n(\mathrm{Si_{oct}})_{\mathrm{ett}} + f_{\mathrm{thaum}} n(\mathrm{Si_{oct}})_{\mathrm{thaum}}$$

where $n(\mathrm{Si_{oct}})$ is the experimentally measured value for the octahedral Si level in the solid, f_{ett} and f_{thaum} are the fractional ratios of ettringite- and thaumasite-like phases in the mixture and $n(\mathrm{Si_{oct}})_{\mathrm{ett}}$ and $n(\mathrm{Si_{oct}})_{\mathrm{thaum}}$ are the limiting compositions on the ettringite and thaumasite sides of the miscibility gap respectively.

This equation was solved using least squares methods for the four two-phase systems to find the best fit values of $n(\mathrm{Si_{oct}})_{\mathrm{ett}}$ and $n(\mathrm{Si_{oct}})_{\mathrm{thaum}}$. This approach gave $n(\mathrm{Si_{oct}})_{\mathrm{ett}} = 1.05$ and $n(\mathrm{Si_{oct}})_{\mathrm{thaum}} = 1.95$.

These limits of miscibility are compared with the initial estimates and with the measurements for the single-phase systems in Fig. 6. On the ettringite side of the miscibility gap, the value of 1.05 agrees well with the initial estimate, again showing that half the Al in ettringite can be replaced by Si.

However, on the thaumasite side of the gap this approach suggests that thaumasite tolerates little or no Al in its structure. The initial estimate suggested a higher level of substitution was possible. Some of the apparently single-phase systems on the thaumasite side of the miscibility gap also suggest higher levels of substitution. We believe that this discrepancy is due to problems with the XRD detection of ettringite in the presence of large amounts of thaumasite in these apparently single-phase systems. Asymmetry in the peak shapes, which leads to higher intensity on the lower angle side of the peaks than on the higher angle side, could potentially lead to significant amounts of ettringite-like phases being undetected in the presence of thaumasite because the ettringite peaks are at slightly lower angles than the equivalent thaumasite peaks. (Conversely, this asymmetry would not cause the same problem in detecting thaumasite in the presence of large amounts of ettringite.) Approximately 10 wt.% ettringite in the single-phase system on the thaumasite side of the miscibility gap would account for the discrepancy between the initial estimate for the limiting composition on the thaumasite side of the gap and our final result.

5. Conclusions

A gap in the solid solution between thaumasite and ettringite can be identified crystallographically by a gap in the unit cell dimensions of the solid solution phases between *c*-dimensions of 20.95(10.475) and 21.3 Å. This gap is believed to correspond to a change in symmetry from the thaumasite structure to the ettringite structure.

The combination of the techniques of quantitative X-ray diffraction and infrared spectroscopy has enabled us to identify the extent of immiscibility in the thaumasite–ettringite system for the first time. Thaumasite can tolerate little or no replacement of Si by Al in its structure.

Ettringite tolerates a higher degree of solid solution, with up to 1/2 its Al being replaced by Si.

This work has highlighted problems in detecting ettringite by XRD in the presence of large amounts of thaumasite. This effect should be considered when analysing cement and concrete samples which have been affected by the thaumasite form of sulfate attack.

The location of the miscibility gap in this system, between 50% and 97% replacement of Al by Si, has implications for the formation of thaumasite in different cement systems. The thaumasite structure can accept only a limited amount of aluminium and therefore equilibrium systems which contain larger amounts of aluminium are unlikely to form a stable thaumasite phase. The chemistry of cements blended with BFS, PFA etc., that contain higher Al levels than OPC, suggests that the formation of a stable thaumasite phase in slag or fly ash blended systems is less likely.

References

[1] Taylor HFW. Cement chemistry. London: Thomas Telford Publishing; 1997.

[2] Report of the Thaumasite Expert Group. The thaumasite form of sulfate attack: risks, diagnosis, remedial works and guidance on new construction. London: Her Majesty's Stationery Office, 1999.

[3] Crammond NJ. Thaumasite in failed cement mortars and renders from exposed brickwork. Cem Concr Res 1985;15:1039–50.

[4] Lachaud R. Thaumasite et ettringite dans les matériaux de construction. Ann l'Inst Bât Trav Publics 1979;32:370–3.

[5] Edge RA, Taylor HFW. Crystal structure of thaumasite $[Ca_3Si(OH)_6 \cdot 12H_2O]SO_4CO_3$. Acta Cryst B 1971;27:594–601.

[6] Struble LJ. Synthesis and characterisation of ettringite and related phases. In: Proceedings of VIIIth International Congress on the Chemistry of Cement 1987, p. 582–8.

[7] Moore AE, Taylor HFW. Crystal structure of ettringite. Acta Cryst B 1970;26:386–93.

[8] Kollmann H, Strubel G. Ettringite–thaumasite mixed crystals of Brenk (Eifel). Chem Erde 1981;40:110–20 [in German].

[9] Kollmann H, Strubel G, Trost F. Mineralsynthetic tests to find the causes of expansion through Ca–Al-sulfate-hydrate and Ca–Si-carbonate-sulfate-hydrate. Tonind-Ztg 1977;101:63–70 [in German].

[10] Barnett SJ, Adam CD, Jackson ARW. Solid solutions between ettringite and thaumasite. J Mat Sci 2000;35(16):4109–14.

[11] Barnett SJ, Macphee DE, Crammond NJ. Solid solutions between thaumasite and ettringite and their role in sulfate attack. Concr Sci Eng 2001;3(12):209–15.

[12] Barnett SJ, Macphee DE, Lachowski EE, Crammond NJ. XRD, EDX and IR analysis of solid solutions between thaumasite and ettringite. Cem Concr Res 2002;32:719–30.

[13] Lachowski EE, Barnett SJ, Macphee DE. Transmission electron optical study of ettringite/thaumasite solid solutions. Paper submitted to First International Conference on Thaumasite in Cementitious Materials.

[14] Larson AC, Von Dreele RB. General structure analysis system (GSAS). Los Alamos National Laboratory Report. LAUR 86-748, 2000.

[15] Tobey BH. Expgui, a graphical user interface for GSAS. J Appl Cryst 2001;34:210–3.

[16] Varma SP, Bensted J. Studies of thaumasite part I. Silic Indus 1973;38:29–32.

[17] Bensted J, Varma SP. Studies of thaumasite part II. Silic Indus 1974;39:11–9.

[18] Perkins RB, Palmer CD. Solubility of $Ca_6[Al(OH)_6]_2(CrO_4)_3 \cdot 26H_2O$, the chromate analogue of ettringite; 5–75 °C. Appl Geochem 2000;15:1203–18.

[19] Perkins RB, Palmer CD. Solubility of ettringite $(Ca_6[Al(OH)_6]_2(SO_4)_3 \cdot 26H_2O)$ at 5–75 °C. Geochim Cosmochim Acta 1999; 63:1969–80.

[20] Hughes TL, Methven CM, Jones TGJ, Pelham SE, Fletcher P, Hall C. Determining cement composition by Fourier transform infrared spectroscopy. Adv Cem Bas Mat 1995;2:91–104.

[21] Farmer VC. The infrared spectra of minerals. London: Mineralogical Society; 1974.